

TRACEABLE DETERMINATION OF MECHANICAL PARAMETERS OF BINOCULAR SHAPED FORCE TRANSDUCERS ACCORDING TO EN ISO 376

M. Kühnel¹, F. Hilbrunner², H. Büchner¹, G. Jäger¹, E. Manske¹ and T. Fröhlich¹

¹Ilmenau University of Technology, Germany, michael.kuehnel@tu-ilmenau.de

²Sartorius Weighing Technology GmbH, Göttingen

Abstract: This paper discusses the traceable determination of mechanical parameters of monolithic binocular shaped dual beam spring elements that are applied as force transducers and load cells in the mass and force metrology. Thereby it mainly deals with the measurement of the specific values creeping, reversibility, reproducibility, zero error and interpolation error which are defined in applicable regulations such as the EN ISO 376 standard or the OIML recommendation R 60. Our determination of those parameters is based on an interferometric deformation measurement of a loaded binocular shaped dual beam spring element which is made of the common aluminum alloy AW 2024. Generally there is no restriction on the spring element material. The parameters mentioned above are derived from the measured interferometer signal according to the EN ISO 376 standard and are thus traceable to the wavelength of light. The used measurement setup is introduced, measurements of the mentioned parameters are presented and their uncertainty is depicted. It is proved that the setup is suitable to classify dual beam spring elements according to the highest accuracy Class 00 of EN ISO 376.

Keywords: creeping, delayed elasticity, hysteresis, reversibility, interpolation error, nonlinearity, zero error, load cell, force transducer, OIML R 60, EN ISO 376

1. INTRODUCTION

In mass and force metrology the deformation measurement of characteristically shaped bodies, so called spring elements, is a common principle to determine forces. There to the force F is acting on the spring element and the generated deformation s or strain ε is measured. Force transducers and load cells with glued on strain gauges are the most common example for this principle. Besides the properties of the strain gauge and the glue layer, the performance of those transducers is highly dependent on the mechanical properties of the spring element. Material imperfections such as the effect of delayed elasticity, nonlinearity and hysteresis of the stress-strain-behavior and the temperature coefficient of the Young's modulus lead to creeping (delayed elasticity), reversibility errors (hysteresis), reproducibility errors, zero point errors and interpolation errors (non-linearity) of the sensor signal as well a temperature dependence of the sensor sensitivity [1]. Those sensor parameters

are evaluated based on the EN ISO 376 (guilty for force transducers) or the OIML R 60 (load cells) [1, 2, 3]. However, the sensor performance can be improved by error compensations and choosing appropriate materials. For this reason exact knowledge and thus an accurate measurement of the described parameters is essential. By measuring the time-, load- and temperature- dependent deformation s of a dual beam spring element under load its parameters named above can be determined definitely and independently from the glued on strain gauges. The evaluation of the parameters in this publication is carried out according to the EN ISO 376 standard. Based on the values defined in this standard, force transducers are classified into four accuracy classes. The classification of the spring elements measured in this work will be done similarly. The requirements of the highest accuracy class (Class 00) are listed in Table 1.

Table 1: maximum relative errors of force transducer in the accuracy Class 00 of EN ISO 376

Parameter	Maximum permissible rel. error in 10^{-5} of Class 00
Creep error $c(t = 3 \text{ min})$	± 25
Reversibility error v	± 70
Reproducibility error b'	± 25
Zero error f_0	± 12
Interpolation Error f_c	± 25

2. MEASUREMENT SETUP

2.1 Principle of the measurements

Monolithic binocular shaped dual beam spring elements are applied as specimen. They are firmly clamped to a frame on one side, see Figure 1. A constant force $F = m \cdot g$ can be loaded to the specimen by applying weights.

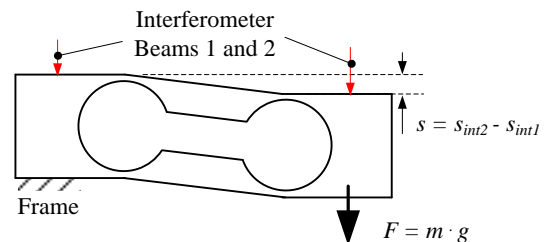


Figure 1: principle of the measurement

The time- and load- dependent deformation $s(t, F)$ is determined as the difference ($s = s_{Int2} - s_{Int1}$) of the two displacement measurements carried out by the use of interferometers. Thus, the measured properties of the spring element and its material are traceable to the wavelength of the used laser light and are independent from the strain gauge properties. If the strain gauge signal is measured at the same time, both signals can be compared and the influence of the strain gauge foil or the glue layer on the strain gauge signal can be investigated.

The differential measurement offers the following benefits: A relative displacement of the specimen to the interferometer (for example caused by temperature changes) does not affect the measurement of the differential deflection s . Furthermore variations of the refractive index of the air due to changes of temperature, humidity or atmospheric pressure become negligible. This enables a very good long term stability of the measurements.

The big advantage of the used binocular shaped spring elements is the extremely low dependence of the deformation on the point of load application. Moreover, the deformed part of the dual beam spring element shifts parallel. Thus, there is almost no tilt of the laser beam reflecting surface, which enables the use of plane mirror interferometers.

2.2 Used measurement setup

The setup basically consists of three levels: The interferometer, the fixture and the load changer. The binocular shaped dual beam spring element under test is clamped in the fixture that is located in the mid-level, see Figure 2.

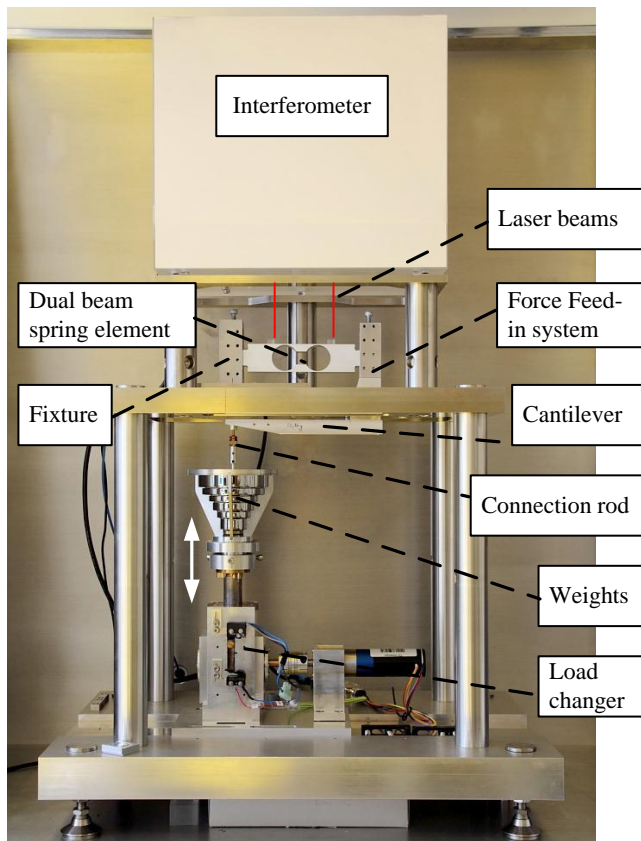


Figure 2: Measurement setup

The fixture consists of a parallel-guided clamp based on the principle of a bench vice. The clamping force is generated by a screw, which is tightened with a defined torque. The force feed-in system is clamped to the dual beam spring element in the same way. A cantilever is mounted on the force feed-in system to introduce the force directly under the fixture. With this structure the lowest contribution of fixture deformations to the measurement uncertainty is achieved, cf. [4]. The connection rod is fixed on the cantilever using a 2-DOF flexure hinge to prevent lateral forces on the dual beam spring element and to ensure, that the center of gravity of the weight is in repeatable position under the fixture. A stack of weights is deposited on the load changer that sits in the lower level. The weights are applied successively to the connection rod and consequently to the specimen by lowering the level of the load changer. The weights (tolerance Class E2 [5]) can be applied to the specimen in the following sequence: 0 g, 50 g, 100 g, 200 g, 300 g, 500 g, and 1000 g.

The generated deformation of the specimen is measured by a Double Plane Mirror Interferometer that is located in the top level of the setup. The Interferometer is made by the SIOS Meßtechnik GmbH in Ilmenau. To reflect the laser beams, the top surface of the dual beam spring element must be polished or mirrors must be attached. The interferometer works on the plane mirror interferometer concept that was developed at the Institute of Process Measurement and Sensor Technology [6]. The resolution is 0.1 nm and the contribution of the interferometer nonlinearity to the measurement uncertainty is in the range of $U_{Lin}^*/s = 0.03 \text{ nm/nm}$ with a maximum of $U_{Lin} = 1 \text{ nm}$ ($k = 1$) whereas s is the corresponding measured length value.

The distance between the two parallel interferometer beams was set to 65 mm. Those beams are focused on the dual beam spring element by the use of lenses. Thus, a tilt of the reflecting mirror does not lead to a tilting of the laser beams inside the interferometer. The whole setup is placed in a climate chamber that was presented in [7]. The temperature stability of the empty chamber is in the range of $\Delta T = \pm 10 \text{ mK}$. The temperature is controlled by a fluid passing through the walls of the chamber. Due to this concept the chamber is mainly free of vibrations and the inner air is static. It is sealed and silica gel is placed inside to keep the relative humidity stable. Static influences of the environmental parameters on the wave length of the laser light are corrected based on the Edlén Formula [8].

The metrological performance and the usability of the setup for the measurement of the delayed elasticity (creep error) of binocular shaped spring elements were proven in [4]. The stability of the length measurement at the given environmental conditions was observed to be better than $\pm 1 \text{ nm/week}$ [4]. This is a fundamental requirement for long term measurements such as the creep error.

2.3 Used specimen

The investigated binocular shaped dual beam spring element (c.f. Figure 3) is made of aluminum AW 2024, which is a standard material for force transducers and load cells [9].

To reduce mechanical stress in the bending zone due to clamping, the bending zone of the dual beam spring element

is separated mechanically from its clamping zones by steps. The laser beam reflecting mirrors are glued on.

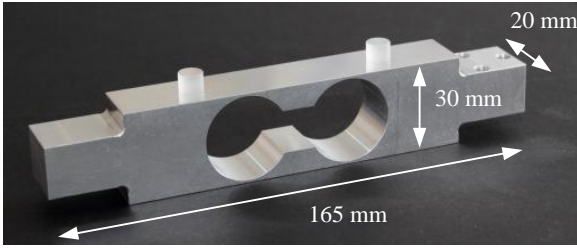


Figure 3: used specimen made of aluminum AW 2024

3. RESULTS

3.1 Preliminary investigations on the setup performance

The relative parameters creep error, reversibility error, reproducibility error, zero error and interpolation error defined in EN ISO 376 consist of an absolute value and are then normalized by the corresponding spontaneous deformation s_0 of the spring element at the given load.

To investigate the contribution of the setup to the measurement uncertainty of those parameters a reference spring element made of fused silica was mounted to the setup. Since the reference spring is a stiff beam, its own deformation is in the range of less than $1\mu\text{m}$ when it is loaded with $m = 1\text{ kg}$. Its outer dimensions are identical with those of the dual beam aluminum spring, cf. Figure 3. Due to the almost perfect mechanical behavior of fused silica, it can be expected, that none of those absolute parameters is exceeding $\pm 0.1\text{ nm}$. If still one of the described errors (such as the creep error) is detected, it will be defined as an uncertainty contribution of the setup to the measurement of the respective parameter. To consider the repeatability of the results the stiff reference spring was mounted four times to the fixture and the measurements were repeated after each assembly. The estimated uncertainty for the measurement of the absolute parameters is listed in Table 2 based on the coverage factor $k = 1$. For each parameter the uncertainty is in the sub nanometer range, whereas U_{fc} is with 0.65 nm the biggest contribution.

Table 2: determined contribution of the measurement setup to the measurement uncertainty of the named parameters if the specimen is loaded with $m \leq 1\text{ kg}$

Parameter	Uncertainty contribution ($k = 1$) the of setup to the measurement of the parameter
Creep error $c(t < 1h)$	$U_c = 0.2\text{ nm}$
Reversibility error v	$U_v = 0.2\text{ nm}$
Reproducibility error b'	$U_{b'} = 0.2\text{ nm}$
Zero error f_0	$U_{f_0} = 0.1\text{ nm}$
Interpolation Error f_c	$U_{fc} = 0.7\text{ nm}$

The contribution of the setup $s_{0,setup}$ to the measured spontaneous deformation s_0 was determined based on a comparison of the measured and a computed deformation. The computed deformation of the stiff reference spring element was calculated with a numerical tool (Ansys) con-

sidering a Young's modulus $E_0 = 75000 \pm 3000\text{ N/mm}^2$ of the fused silica spring. In consequence the contribution of the setup to the spontaneous deformation appears to be $s_{0,setup}/m = -231.3\text{ nm/kg} \pm 20\text{ nm/kg}$ ($k = 1$). The prospective measurements of the spontaneous deformations will be corrected with this value under consideration of the uncertainty contribution $U_{s_0} = 20\text{ nm}$ ($k = 1$).

3.2 Creep error of the aluminum spring element

The measured time and load dependent deformation $s(t)$ of the binocular shaped spring element is shown in Figure 4. The measurements were repeated five times in a row, all within a temperature of $T = 19.58\text{ }^\circ\text{C} \pm 0.01\text{ }^\circ\text{C}$. The temperature was measured with a PT 100 resistance thermometer. A loading time of one hour was chosen and the pause time between each of the five load cycles was set to 3.5 hours to reduce the influence of the prior load cycle on the current measurement.

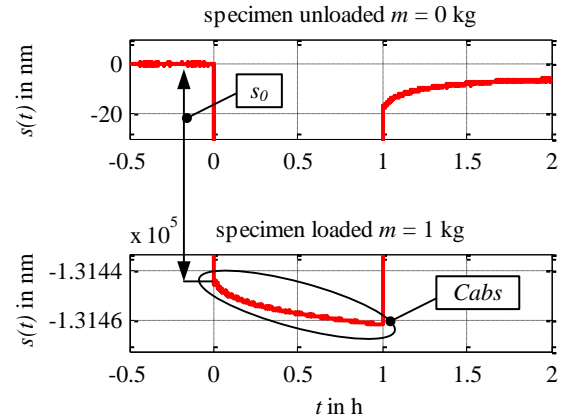


Figure 4: measured deformation of the aluminum spring element

Based on those five measurements a mean value of the time dependent relative creep error $c(t)$ was determined. The resulting curves for both the loading and the unloading cycle are shown in Figure 5 (assembly 1, red curves) corresponding to a coverage factor of $k = 2$. For an investigation of the repeatability of those results the aluminum dual beam spring element was dismantled and mounted another two times and the described measurements were repeated, cf. Figure 4 blue and green curves (assembly 2 and assembly 3). The loading curves have a positive sign because they are normalized with a negative spontaneous deformation.

The difference between the loading and the unloading curves is due to chosen load cycle and the material properties: The current creeping curve is always dependent on the previous loads. In our experiments, the spring was always loaded after a steady state of the deformation was reached. In contrast to that the unloading was always done after one hour of loading whereas no steady state of the deformation existed. If the loading lasts until a steady state of the loading curve is reached, the unloading curve should be equal to unloading curve. Another possibility to achieve equal loading and unloading curves is to perform a cyclical and symmetrical loading and unloading with no pause time between. That means for example: 1hour loading, 1 hour unloading,

1 hour loading and so on. After some of those cycles the curves approach more and more to a common value.

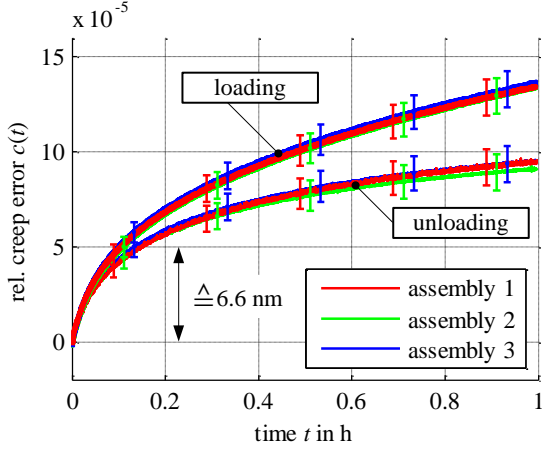


Figure 5: creep error of the aluminum spring element measured based on 3 consecutive assemblies

The calculation of the measurement uncertainty of c was carried out based on the following equations, whereas C_{abs} is the absolute creeping in nm:

$$c = \frac{C_{abs}}{s_0} \quad (1)$$

Consequently the uncertainty can be expressed as:

$$U = \sqrt{\left(\frac{1}{s_0} U_{C_{abs}}\right)^2 + \left(\frac{C_{abs}}{s_0^2} U_{s_0}\right)^2} \quad (2)$$

The uncertainty $U_{C_{abs}}$ consists of the contribution of the interferometer nonlinearity U_{Lin} , the setup U_c and the standard uncertainty U_σ of the 5 measurements of C_{abs} :

$$U_{C_{abs}} = \sqrt{U_c^2 + U_{Lin}^2 + U_\sigma^2} \quad (3)$$

The standard uncertainty U_σ considers random influences such as fast and not correctable variations of the environmental parameters. With $C_{abs} = 17.6$ nm (absolute creeping after one hour of loading) the maximum contribution of the nonlinearity is:

$$U_{Lin} = \frac{U_{Lin}^*}{s} \cdot C_{abs} = 0.03 \frac{\text{nm}}{\text{nm}} \cdot 17.6 \text{ nm} = 0.53 \text{ nm} \quad (k=1)$$

For smaller C_{abs} , the overall uncertainty is lower, cf. above. With $U_c = 0.3$ nm, $U_\sigma = 0.26$ nm, $U_{s_0} = 20$ nm and the spontaneous deformation $s_0 = 131443.2$ nm the overall uncertainty for the creeping error results in $U = 1 \cdot 10^{-5}$ ($k=2$). This value is true for the maximum C_{abs} at $t = 1$ h. The contribution of the spontaneous deformation is in the range of just 10^{-8} and can be neglected in further calculations.

A very good repeatability of the measurements of the three consecutive assemblies was achieved. The curves are identical within the limits of the estimated uncertainty. That proves the perfect setup applicability for the measurements of the creeping error of those dual beam spring elements.

Finally the rel. creep error of the aluminum dual beam spring after one hour of loading can be given as $c(t=1h) = 1.35 \cdot 10^{-4} \pm 0.1 \cdot 10^{-4}$ ($k=2$). Thus, the measured creep error after one hour of loading is even smaller than the permissible creep error after three minutes of loading, cf. Table 1.

3.3 Further parameters according to EN ISO 376

Afterwards the parameters rel. reversibility error, rel. reproducibility error, rel. zero error and rel. interpolation error of the aluminum spring were determined according to the EN ISO 376 standard [2]. Thereto the spring element was loaded stepwise with a maximum load of $m = 1$ kg, see Figure 6 a). Each step was held for 1 minute. For statistical issues the shown load cycle was repeated six times with a pause time of 3 minutes between each cycle. Furthermore those measurements were repeated another two times after the spring element was dismounted and mounted again (assembly 1-3, cf. capture 3.2).

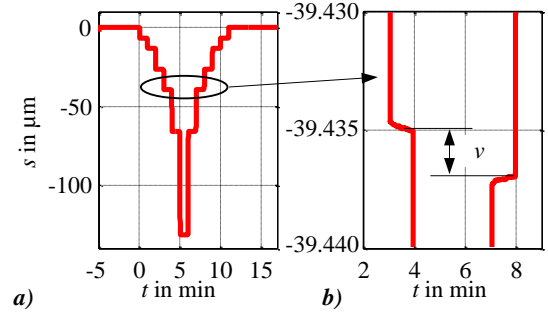


Figure 6: a) Deformation s of the aluminum dual beam spring when the load is applied stepwise b) s at $m = 300$ g; v indicates the absolute reversibility error at this point

Relative reversibility error v

The rel. reversibility error derived from the measurements is shown in Figure 7. Due to the normalization with the spontaneous deformation of the according load step its maximum and the maximum of the uncertainty appears at the lowest load $m = 50$ g with $v = 2.45 \cdot 10^{-4} \pm 0.75 \cdot 10^{-4}$ ($k=2$) which corresponds to an absolute value of $1.6 \text{ nm} \pm 0.5 \text{ nm}$. Finally, the rel. reversibility error of the aluminum dual beam spring can be summarized with $v < 3.2 \cdot 10^{-4}$ ($k=2$).

The calculation of the uncertainty was done based on the procedure described in section 3.2 considering the standard uncertainty U_σ of the six measurements, the contribution of the setup U_v (cf. Table 2) and the interferometer nonlinearity U_{Lin} .

Comparing the results of the three assemblies a very good repeatability of the measurements was achieved here as well. The difference between the measured curves is less than $1 \cdot 10^{-5}$.

Reproducibility error b'

The maximum reproducibility error was measured to be $b' = 7.4 \cdot 10^{-5} \pm 6.9 \cdot 10^{-5}$ ($k=2$) and thus in somewhat simplified terms $b' < 14.3 \cdot 10^{-5}$ ($k=2$), cf. Figure 8. A very good repeatability of the three measurements was observed here

again. The difference between the three assemblies is less than $1 \cdot 10^{-6}$. The given uncertainty bases on U_σ , $U_{b'}$ and U_{Lin} .

Zero error f_0

The zero error is normalized by the maximum deformation and was determined to be $f_0 = 9.3 \cdot 10^{-6} \pm 4 \cdot 10^{-6}$ ($k = 2$) and thus $f_0 < 13.3 \cdot 10^{-6}$ ($k = 2$). The estimated uncertainty bases on U_σ , U_{f_0} and U_{Lin} .

Interpolation error f_c

The interpolation error was computed based on a degree one polynomial (straight line) and is depicted in Figure 9. Except the value at $m = 50$ g of assembly 1 the error is smaller than $1 \cdot 10^{-5}$. However, due to the large relative measurement uncertainty it must be indicated to be $f_c < 5 \cdot 10^{-4}$ ($k = 2$), even though the performance of the spring element seems to be much better. The estimated uncertainty bases on U_σ , U_{f_c} and $U_{Lin} = 1$ nm ($k = 1$).

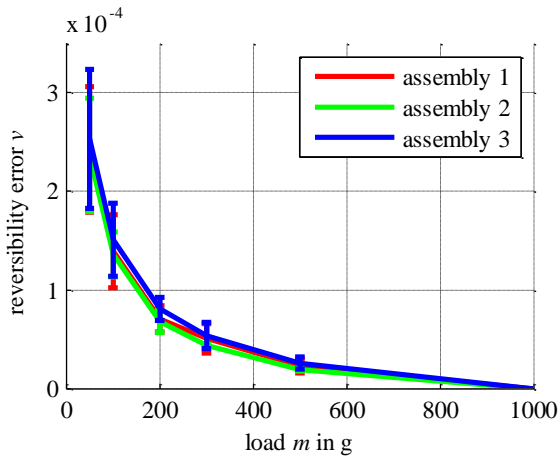


Figure 7: relative reversibility error ν in the whole measurement range from $50 \text{ g} \leq m \leq 1000 \text{ g}$

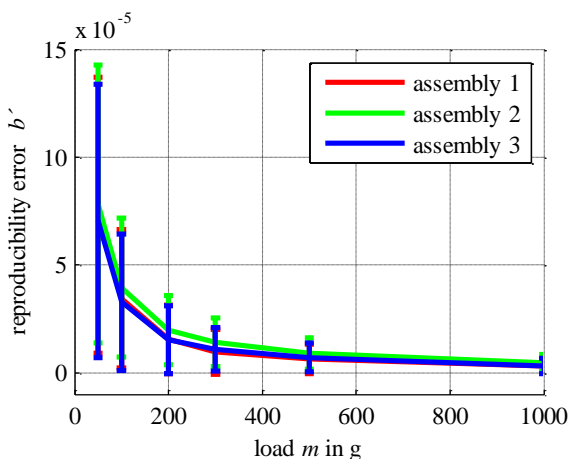


Figure 8: relative reproducibility error b' in the whole measurement range from $50 \text{ g} \leq m \leq 1000 \text{ g}$

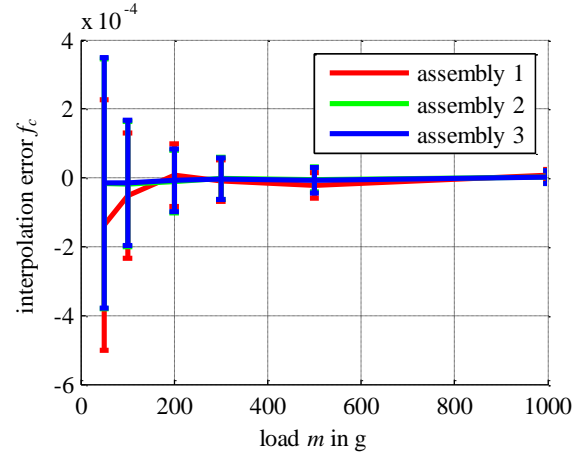


Figure 9: relative interpolation error f_c in the whole measurement range from $50 \text{ g} \leq m \leq 1000 \text{ g}$

4. SUMMARY AND CONCLUSIONS

A summary of the determined mechanical parameters of the aluminum dual beam spring is given in Table 3.

Table 3: maximum relative errors of the aluminum dual beam according to EN ISO 376

Parameter	Maximum rel. error in 10^{-5} of Class 00
Creep error $c(t = 1 \text{ h})$	< 14.5
Reversibility error ν	< 32
Reproducibility error b'	< 14.3
Zero error f_0	< 1.4
Interpolation Error f_c	< 50

Except for the interpolation error, the values accomplish the requirements of the highest accuracy Class 00 of the EN ISO 376 standard. Based on those measurements this aluminum dual beam spring is very well suited for force measurement applications. Since both the used material and the dual beam shape are common standards in the mass and force metrology the low relative errors were expected.

Considering those results, the estimated uncertainties and the repeatability of the measurements the presented setup is perfectly suited for a high precision determination of the mechanical parameters creeping, reversibility, reproducibility and zero error of common dual beam spring elements according to EN ISO 376. This is achieved because the uncertainty contribution of the setup to the measurement of the corresponding absolute parameters is in the sub nanometer range.

In contrast to that, the nonlinearity of the interferometer of just 1 nm ($k = 1$) significantly limits the measurement of the interpolation error of the spring element. Thus, a classification of the spring elements interpolation error f_c in the highest accuracy class of EN ISO 376 is not possible. A fivefold improvement of the interferometer nonlinearity can be achieved by applying a Heydemann correction on the interferometer signals. With the resulting interferometer nonlinearity of < 0.2 nm [10] the determination of the

interpolation error would be precisely enough to fulfill the requirements of EN ISO 376 Class 00.

Since the measurement procedure and the data evaluation are similar, the presented setup is also suitable for the classification of load cells according to OIML R60. Here, the described measurements have to be carried out at constant temperatures of $T = -10\text{ °C}$, $T = 20\text{ °C}$ and $T = 40\text{ °C}$. This can be realized with the applied climate chamber.

Moreover it is possible to measure dual beam spring elements with other dimensions or made from different materials than aluminum. Measurements on this will be carried out in the future.

Beyond that, it will be possible to mount a complete strain gauge based force transducer to the setup and measure its strain gauge signal and the shown deformation signal at the same time and compare both results. Thus, the influence of the glue layer, the carrier foil and the sealings can be investigated as well.

5. ACKNOWLEDGEMENTS

The authors thank all the colleagues of the Institute of Process Measurement and Sensor Technology who contributed to the development of the presented setup. The setup was designed within the projects “SensoPlas”, supported by the Association of German Engineers (VDI), and “Innovative Kraftmess- und Wägetechnik”, supported by the Federal Ministry of Education and Research (BMBF) in cooperation with Sartorius Weighing Technology GmbH and SIOS Meßtechnik GmbH.

6. REFERENCES

- [1]: Roman Schwartz: Handbuch der Mess- und Automatisierungstechnik in der Produktion, Teil B, S. 55-92, editor: Gevatter, Hans-Jürgen; Grünhaupt, Ulrich; Springer Verlag; ISBN-13: 978-3-540-21207-2; 2006
- [2]: EN ISO 376:2011: Metallic materials. Calibration of force-proving instruments used for the verification of uniaxial testing machines (ISO 376:2011);
- [3]: OIML R 60: International Recommendation, Edition 2004 (E): Metrological regulation for load cells
- [4]: M. Kühnel, F. Hilbrunner, H. Büchner, G. Jäger, T. Fröhlich: Traceable determination of relevant material parameters for the mass and force metrology; Proceedings of the 2011 NCSL International Workshop and Symposium, Washington D.C.
- [5]: OIML R 111: International Recommendation, Edition 2000 (E): Weights of classes E1, E2, F1, F2, M1, M1-2, M2, M2-3 and M3 Part 1: Metrological and technical requirements
- [6]: Büchner, H-J.; Jäger, Gerd: A novel plane mirror interferometer without using corner cube reflectors; Meas. Sci. Technol. 17 (2006) 746–752
- [7]: Kühnel, M; Hilbrunner, F; Fröhlich, T; Lieberherr, K: Climate Chamber for a high temperature stability; SENSOR 2011, Nürnberg, 15th International Conference on Sensors and Measurement Technology
- [8]: Edlén B.: The Refractive Index of Air, Metrologica, Bd. 2, Nr. 2, pp. 71-80, 1966.
- [9]: Hannah, R.L.; Reed, S. E.: Strain Gauge Users Handbook
- [10]: Manske, E.; Lichtwellenleitergekoppelte Miniaturinterferometer für die Präzisionsmesstechnik, Habilitation, Ilmenau, 2005